Geothermal Energy Engineering

Exploration, Extraction and Usage

Kale Stewart

SYRAWOOD
PUBLISHING HOUSE

Geothermal Energy Engineering: Exploration, Extraction and Usage

About the Book

This book provides comprehensive insights into the field of geothermal energy engineering. It explores all the important aspects of this field in the present day scenario. Geothermal energy is one of the most important forms of alternative energy present today. It is generated within earth's crust because of radioactive decay of materials and is stored in the same. It is the most reliable, cost-effective and environmental friendly power. This text will give detailed analysis about the use and extraction of geothermal energy. It will also discuss the engineering methods required for its exploration. Different approaches, evaluations, methodologies and advanced studies in this area have been included in the text. Students, researchers, experts and all associated with the field of geothermal energy engineering will benefit alike from this text.

About the Editor

Kale Stewart pursued his Post Graduate Certificate in Geothermal Energy Technology from the University of Auckland, New Zealand. Stewart's academic interests lie in thermal energy, geothermal power and geothermal heating. Stewart is a renowned lecturer of undergraduate programs and travels extensively for educating students across the globe. He has authored and edited several texts, which include articles, technical papers and book chapters, in the fields of enhanced geothermal systems, geothermal gradient and thermal energy storage.

SYRAWOOD
PUBLISHING HOUSE
www.syrawoodpublishinghouse.com

ISBN 978-1-68286-462-3
90000
9 781682 864623

Stewart

Geothermal Energy Engineering: Exploration, Extraction and Usage

SYRAWOOD PUBLISHING HOUSE

Geothermal Energy Engineering: Exploration, Extraction and Usage

Edited by Kale Stewart

SYRAWOOD
PUBLISHING HOUSE
New York

Published by Syrawood Publishing House,
750 Third Avenue, 9th Floor,
New York, NY 10017, USA
www.syrawoodpublishinghouse.com

Geothermal Energy Engineering: Exploration, Extraction and Usage
Edited by Kale Stewart

© 2017 Syrawood Publishing House

International Standard Book Number: 978-1-68286-462-3 (Hardback)

This book contains information obtained from authentic and highly regarded sources. Copyright for all individual chapters remain with the respective authors as indicated. All chapters are published with permission under the Creative Commons Attribution License or equivalent. A wide variety of references are listed. Permission and sources are indicated; for detailed attributions, please refer to the permissions page and list of contributors. Reasonable efforts have been made to publish reliable data and information, but the authors, editors and publisher cannot assume any responsibility for the validity of all materials or the consequences of their use.

The publisher's policy is to use permanent paper from mills that operate a sustainable forestry policy. Furthermore, the publisher ensures that the text paper and cover boards used have met acceptable environmental accreditation standards.

Trademark Notice: Registered trademark of products or corporate names are used only for explanation and identification without intent to infringe.

Cataloging-in-publication Data

Geothermal energy engineering : exploration, extraction and usage / edited by Kale Stewart.
p. cm.
Includes bibliographical references and index.
ISBN 978-1-68286-462-3
1. Geothermal engineering. 2. Geothermal resources. I. Stewart, Kale.
TJ280.7 .G46 2017
621.44--dc23

Printed in the United States of America.

此为试读，需要完整PDF请访问：www.ertongbook.com

Geothermal Energy Engineering: Exploration, Extraction and Usage

PREFACE

This book provides comprehensive insights into the field of geothermal energy engineering. It explores all the important aspects of this field in the present day scenario. Geothermal energy is one of the most important forms of alternative energy present today. It is generated within earth's crust because of radioactive decay of materials and is stored in the same. It is the most reliable, cost-effective and environmental friendly power. This text will give detailed analysis about the use and extraction of geothermal energy. It will also discuss the engineering methods required for its exploration. Different approaches, evaluations, methodologies and advanced studies in this area have been included in the text. Students, researchers, experts and all associated with the field of geothermal energy engineering will benefit alike from this text.

This book has been an outcome of determined endeavour from a group of educationists in the field. The primary objective was to involve a broad spectrum of professionals from diverse cultural background involved in the field for developing new researches. The book not only targets students but also scholars pursuing higher research for further enhancement of the theoretical and practical applications of the subject.

It was an honour to edit such a profound book and also a challenging task to compile and examine all the relevant data for accuracy and originality. I wish to acknowledge the efforts of the contributors for submitting such brilliant and diverse chapters in the field and for endlessly working for the completion of the book. Last, but not the least; I thank my family for being a constant source of support in all my research endeavours.

Editor

TABLE OF CONTENTS

Preface VII

Chapter 1 **Effectiveness of acidizing geothermal wells in the South German Molasse Basin** 1
S. Schumacher and R. Schulz

Chapter 2 **Convective, intrusive geothermal plays: what about tectonics?** 12
A. Santilano, A. Manzella, G. Gianelli, A. Donato, G. Gola, I. Nardini, E. Trumpy and S. Botteghi

Chapter 3 **Stored-heat assessments: a review in the light of field experience** 21
M. A. Grant

Chapter 4 **Proposal of a consistent framework to integrate geothermal potential classification with energy extraction** 27
G. Falcone

Chapter 5 **Reservoir characterization of the Upper Jurassic geothermal target formations (Molasse Basin, Germany): role of thermofacies as exploration tool** 32
S. Homuth, A. E. Götz and I. Sass

Chapter 6 **Empirical relations of rock properties of outcrop and core samples from the Northwest German Basin for geothermal drilling** 41
D. Reyer and S. L. Philipp

Chapter 7 **Geochemical study on hot-spring water in West New Britain Province, Papua New Guinea** 58
M. M. Lahan, R. T. Verave and P. Y. Irarue

Chapter 8 **Overcoming challenges in the classification of deep geothermal potential** 65
K. Breede, K. Dzebisashvili and G. Falcone

Chapter 9 **Thermodynamic and thermoeconomic analysis of combined geothermal space heating and thermal storage using phase change materials** 86
V. Chauhan and Á. Ragnarsson

Chapter 10 **Assessing the prospective resource base for enhanced geothermal systems in Europe** 98
J. Limberger, P. Calcagno, A. Manzella, E. Trumpy, T. Boxem, M. P. D. Pluymaekers, and J.-D. van Wees

Chapter 11 **Influence of major fault zones on 3-D coupled fluid and heat transport for the Brandenburg region (NE German Basin)** 115
Y. Cherubini, M. Cacace, M. Scheck-Wenderoth and V. Noack

Chapter 12 **Geothermal heat pump system assisted by geothermal hot spring** 135
M. Nakagawa and Y. Koizumi

Chapter 13 **Geothermal resources and reserves in Indonesia: an updated revision** 145
A. Fauzi

Chapter 14 **Rearrangement of stresses in fault zones – detecting major issues of coupled hydraulic–mechanical processes with relevance to geothermal applications** 151
G. Ziefle

Chapter 15 **Geothermometric evaluation of geothermal resources in southeastern Idaho** 161
G. Neupane, E. D. Mattson, T. L. McLing, C. D. Palmer, R. W. Smith, T. R. Wood and R. K. Podgorney

Permissions

List of Contributors

Index

此为试读，需要完整PDF请访问：www.ertongbook.com

1

Effectiveness of acidizing geothermal wells in the South German Molasse Basin

S. Schumacher and R. Schulz

Leibniz Institute for Applied Geophysics, Stilleweg 2, 30655 Hanover, Germany

Correspondence to: S. Schumacher (sandra.schumacher@liag-hannover.de)

Abstract. In Germany, many hydro-geothermal plants have been constructed in recent years, primarily in the region of Munich. As the host formation here mainly consists of carbonates, nearly all recently drilled wells have been acidized in order to improve the well yield. In this study, the effectiveness of these acid treatments is analyzed with respect to the amount of acid used and the number of acid treatments carried out per well. The results show that the first acid treatment has the largest effect, while subsequent acidizing improves the well only marginally. Data also indicate that continued acidizing can lead to degradation of the well. These findings may not only be important for geothermal installations in Germany but also for projects, for example, in Austria, France or China where geothermal energy is produced from carbonate formations as well.

1 Introduction

1.1 Geothermal energy in Germany

The growing need for energy and the rising prices of conventional energy sources such as oil, gas and coal have led to increased interest and investment in environmentally friendly, renewable energy in Germany. One such renewable resource is geothermal energy, which, compared to other more widespread resources such as wind or solar energy, has the tremendous advantage of being able to deliver heat and electrical energy independent of weather conditions and time of day.

In Germany, large geothermal plants require the use of deep geothermal energy, which so far has only been used in the form of hydro-geothermal energy (Schellschmidt et al., 2010). For this kind of energy, certain requirements have to be fulfilled, such as the existence of an aquifer of hot water. Hence, the generation of hydro-geothermal energy in Germany is mainly confined to three areas: the North German Basin, the Upper Rhine Graben and the South German Molasse Basin. The Molasse Basin (specifically the region of Munich) has become the center of geothermal energy production in Germany within the last few years due to favorable geological conditions.

1.2 Geological setting

In the Molasse Basin, hot water can be found in the stratigraphic unit of the Malm aquifer (Upper Jurassic). The sedimentary layers of the karstic Malm aquifer primarily consist of carbonate rocks, namely small-pored white limestones as well as fine-to-coarse crystalline dolomites (e.g., Wolfgramm et al., 2007). For the well Pullach Th2, pure limestones as well as limestone layers that contain clay in varying degrees have been described (Böhm et al., 2010), while Reinhold (1998) identifies oolitic platform sands with associated mounts of microbe–siliceous sponges in the Upper Jurassic of the Swabian Alb (Swabian facies). These variations in material can be explained by the different facies that can be encountered in the Malm aquifer. Facies found in the Malm aquifer encompass the Swabian, the Franconian, and the Helvetic facies.

The Helvetic facies developed under distal conditions and as a consequence contains not only carbonates but also a significant amount of marls (Meyer and Schmidt-Kaler, 1996). Therefore, it exhibits only very small transmissivities (Villinger, 1988; Bayerisches Staatsministerium für Wirtschaft, Infrastruktur, Verkehr und Technologie, 2010). Although the Helvetic facies is restricted to the southwestern part of the basin, small transmissivities are not restricted to the Helvetic facies itself but are also found in areas adjacent

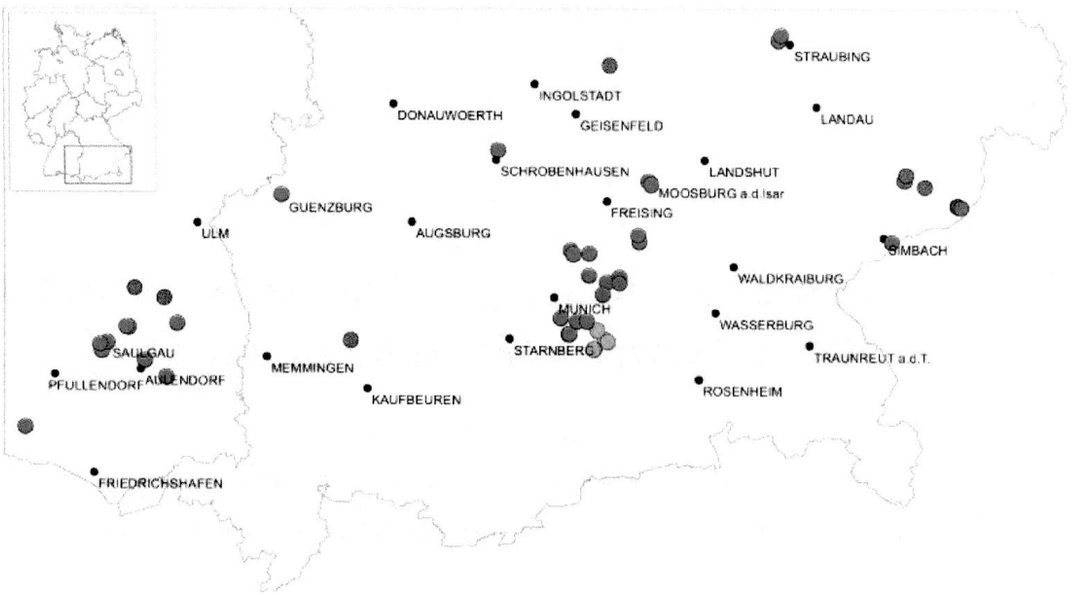

Figure 1. A map of southern Germany and geothermal installations within the Malm aquifer. Main uses are district heating (red dots), power generation (blue dots), and spas (gray dots).

to it (Stober and Villinger, 1997), which can be explained by a lack of karstification (Villinger, 1997).

The Franconian facies, found in the region of Munich, developed in a shelf environment. It contains basin facies and reef facies. While the basin facies consists of banked limestones, which were deposited in shallow waters between reefs, the carbonates of the reef facies are built up by reef detritus. Thus, the matrix porosity of the reef facies tends to be higher than that of the other facies. As a result, recrystallization of limestone into dolomite primarily takes place in the reef facies (e.g., Bausch, 1963). Dolomites are characterized by a predominantly good porosity caused by the reduction in volume due to the dolomitization of limestone (Koch, 1997), which can result in an increase in porosity by up to 13 % (Böhm et al., 2011). Therefore, the reef facies in the Molasse Basin is of special interest for the planning of geothermal projects.

In addition to matrix porosity, pathways for fluid flow that have been created by karstification play a dominant role within the Malm aquifer. As a result, transmissivity is higher in the north of the basin than in the south, since rocks in the north underwent a higher rate of karstification than those in the south, where the transmissivity depends mainly on the matrix porosity of the carbonates (Koch and Sobott, 2005) and on fissures (Wolfgramm et al., 2009). Analysis of pump tests shows that transmissivities within the Malm aquifer vary by more than seven orders of magnitude (Birner et al., 2012). However, in the region of Munich, which is of special interest for this study due to the high number of geothermal wells in this area, transmissivities change by only two orders of magnitude (Birner et al., 2012).

It is also important to note that the water within the Malm aquifer shows only low mineralization (e.g., Prestel, 1990; Wolfgramm and Seibt, 2008) despite the fact that this water has been buried to significant depths for long periods. Prestel (1990), for example, gives an age of 6700 to 10 400 yr for water encountered in the well Saulgau GB3 (for approximate location see Fig. 1, "Saulgau"), dating it to the Holocene. Bertleff and Watzel (2002) state that water in the basin's center is of Pleistocene age. In general, water tends to be younger toward the borders of the basin, but it has been found that the mineral load is low even at the center. Because of this, water within the Malm aquifer is a perfect repository for hydrogeothermal energy use.

1.3 Technical details

The geologic setting is important for the exploitation of geothermal energy in the Molasse Basin as not only is a high transmissivity needed in order to operate geothermal power plants economically, but high temperatures are also essential. As a general trend, it can be observed that with increasing depth of the Malm aquifer to the south, temperatures found within this layer also increase. This, however, is contrary to the behavior of the transmissivity, which tends to decrease to the south (Birner et al., 2012).

In the region of Munich, both parameters were assumed to exhibit values suitable for the exploitation of geothermal energy for district heating and/or electricity generation. Therefore, in recent years many geothermal plants have been constructed in this area. In order to increase the yield of the wells and therefore their economic efficiency, acidizing has been performed on nearly all of these wells. The primary acid used was hydrochloric acid in varying dilutions, but in some cases small amounts of citric and acetic acid were also used

as admixing. In this work the effectiveness of these acid treatments has been analyzed based on data from 17 wells.

1.4 Data origin

In Germany, operators of geothermal plants are legally obligated to pass on information about stimulation procedures and pump tests to the responsible state geological survey. However, they are not required to go into detail or to give access to the original measurements. In general, the results of pump test analyses done by service companies are reported. Depending on the service company, these reports include details about the duration of the stimulation measure or the part of the well acidized, but often only the bare minimum (such as flow rate and specific capacity, i.e., flow rate divided by drawdown) is included.

As part of the research project "Geothermal Information System for Germany" (GeotIS), access to the information of the state geological surveys was granted, which enabled this metaanalysis of acidizing data. However, this meant that none of the original pump test measurements and only limited information about their analysis was available. Therefore, this paper deals only with the most basic data, which are routinely acquired by operators of geothermal plants. This has the advantage that future geothermal projects do not need to deviate from standard procedures in data acquisition and analysis in order to use the insights gained from this work.

2 Theory of laminar and turbulent flow

Fluid flow into a well is defined by Darcy's law.

$$Q = k \cdot A \cdot i \tag{1}$$

with Q being the flow rate [$m^3\,s^{-1}$], k the coefficient of permeability or hydraulic conductivity [$m\,s^{-1}$], A the surface area through which the fluid passes [m^2], and i is the hydraulic gradient [1]. Under the assumption that the water enters the well perpendicular to the well's axis through parts of the uncemented regions of the borehole, Eq. (1) can be rewritten as

$$Q = 2\pi r H k \frac{\mathrm{d}h}{\mathrm{d}l}, \tag{2}$$

where r is the radius of the borehole [m], H the thickness of the aquifer [m], and $\mathrm{d}h/\mathrm{d}l$ is the gradient of the water table or piezometric surface [1] (Hamill and Bell, 1986; Hölting and Coldewey, 2009). It is therefore apparent that the flow rate depends linearly on the hydraulic conductivity of the surrounding rock. In the case of a karst aquifer, such as the Malm aquifer, the hydraulic conductivity of the immediate surroundings may be small due to a lack of fissures and fractures, and therefore impeding a high flow rate. The overall hydraulic conductivity of the aquifer, however, may be comparatively high and well-suited for geothermal exploitation. Thus, the idea of acidizing is to improve the connection of the well to fissures and fractures in its immediate surroundings, and to widen those in order to enhance the well's flow rate.

The theory of fluid dynamics has shown that the transition from laminar to turbulent flow in a pipe occurs at a Reynolds number Re between about 2200 (Turcotte and Schubert, 2002) and 2300 (Schlichting and Gersten, 2001), with Re [1] being defined as

$$Re = \frac{\rho \cdot v \cdot D}{\mu}, \tag{3}$$

where ρ is the fluid's density [$kg\,m^{-3}$], D the diameter of the borehole [m], and μ the fluid's dynamic viscosity [Pa s]. The critical velocity for the onset of turbulence for boreholes considered in this study can be calculated to be in the range of about 0.002 to 0.010 $m\,s^{-1}$. This is far below the velocity of about 1.4 $m\,s^{-1}$ that is obtained for a flow rate of 50 $L\,s^{-1}$, which is a typical flow rate for the wells considered in this analysis. Fully developed turbulent flow can be assumed to take place for $Re > 5000$ (Spurk, 2006). As the Reynolds numbers for all wells are larger than 400 000, it can be concluded that all wells operate within the fully turbulent regime.

Pump tests are a combination of an aquifer test and a well test. Flow within the aquifer is assumed to be laminar, while it is assumed to be turbulent within the well and its immediate surroundings. In previous modeling of the Malm aquifer in the region of Munich, it has been shown that the pressure conditions within the aquifer can be simulated using a porous matrix with laminar flow instead of a karst model (Bartels et al., 2012; Bartels and Wenderoth, 2012), which can also exhibit turbulent flow. The porous matrix model has been calibrated against well test data as well as data from operating geothermal plants, and a good correlation between measured and modeled data has been achieved. Thus, the assumption of laminar flow within the Malm aquifer for large-scale considerations seems justified. The assumption of turbulent flow within the well and its surroundings has been shown above to be correct for the wells considered in this analysis. Therefore, the equation proposed by, for example, Jacob (1947) and Hamill and Bell (1986) for the drawdown in the well can describe this behavior mathematically:

$$s = BQ + CQ^2, \tag{4}$$

where s is the drawdown [m], Q the flow rate [$m^3\,s^{-1}$], and B and C coefficients with units of [$s\,m^{-2}$] and [$s^2\,m^{-5}$], respectively. The drawdown can be described either by the height difference of the water column in the well or by the pressure difference that is caused by changes in water column height and that is measured by a pressure gauge within the well. In the latter case, the unit of drawdown changes to [MPa], with the units of B and C changing accordingly. The term BQ describes the aquifer loss, while CQ^2 is the well loss. However, this equation has been derived from experimental data,

and Rorabaugh (1953) argues that the exponent of CQ^2 can vary as it depends on the well efficiency.

In this case, the well loss can be more generally expressed as CQ^p, where p is the exponent as determined by well efficiency, and varies between 1.5 and 3.5. The specific capacity S_c in [$m^2\,s^{-1}$] or [$m^3\,s^{-1}\,MPa^{-1}$] can then be determined by the following equation:

$$S_c = \frac{Q}{s} = \frac{1}{B + CQ^{(p-1)}}. \tag{5}$$

It becomes apparent that the specific capacity of a well decreases with increasing flow rate independent of the mathematical approach used for the well loss. The reason for this is that the water loses kinetic energy due to friction that already occurs in the laminar regime. Turbulence introduces yet another element into the analysis of the fluid flow. As long as the well operates within the laminar regime, the viscosity of the water mainly depends on its temperature. In the turbulent regime, however, eddies within the water lead to the so-called "eddy viscosity", which describes the apparently higher viscosity because of a transfer of kinetic energy to internal energy of the fluid (Schlichting and Gersten, 2001). Because of this and other smaller effects, turbulence introduces more complexity into the calculations and has to be considered in separate terms.

3 Data set and normalization

For many wells acidizing took place in several steps with interposed pump tests. Moreover, a large number of pump tests were carried out as step drawdown tests. The result of this combination can be seen in Fig. 2, where all available data for step drawdown tests are displayed.

Figure 2 shows that the specific capacity is reduced if the flow rate is increased. In this and all following figures, the same symbols and the same well numbers signify the same borehole, while the same colors are indicators of the same acidizing step. The reduction of the specific capacity occurs because a higher flow rate also means a higher velocity of the water within the well and its surroundings, which leads to turbulence for all wells considered in this analysis.

The decrease in specific capacity makes it harder to compare the results of pump tests. Most pump tests were done at different flow rates (see Fig. 2), so due to the effect described above, their results cannot be directly compared, but need to be normalized. In order to achieve this, a linear equation was established for each borehole and acidizing step, describing the decrease in specific capacity with increasing flow rate. The validity of assuming a linear equation is shown in Fig. 2, where especially the long-time pump tests indicate a linear decrease of the specific capacity for the range of flow rates analyzed. For the area of Munich, 23 data sets were available, which contained more than one pump test per acidizing step and for which a linear equation could be found. The resulting slopes of these equations were then averaged so as to

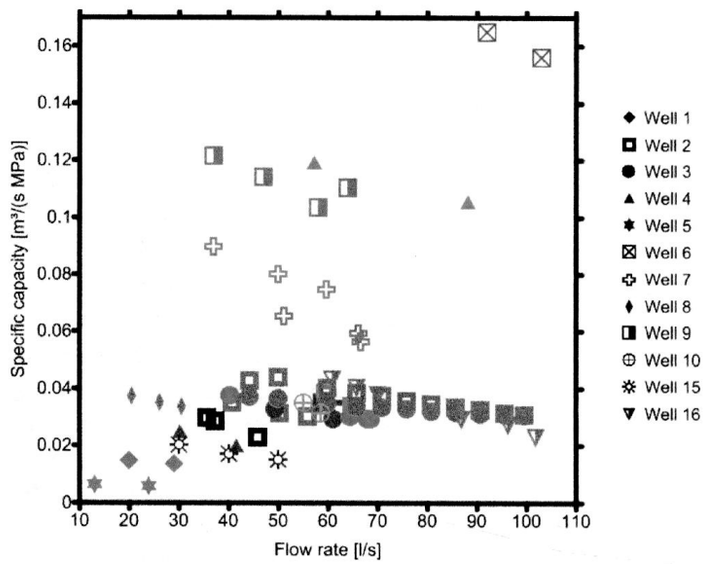

Figure 2. Data used to calculate linear equation for the reduction of the specific capacity with increasing flow rate. Colors indicate the time when the pump tests were performed: before first acid treatment (black), after first acid treatment (green), after second acid treatment (blue), after third acid treatment (red), after fourth acid treatment (orange), after fifth acid treatment (pink), after sixth acid treatment (brown), and long-time pump tests (gray).

use a common value for all further calculations. The resulting linear equation for normalization is

$$S_{c_{norm}} = -0.438\,MPa^{-1} \cdot Q + y, \tag{6}$$

where $S_{c_{norm}}$ is the normalized specific capacity and y the intercept with the ordinate, which has been determined for each acidizing step and borehole beforehand. In principle, it would have been better if each borehole and acidizing step were normalized based on its own linear equation. This, however, was not feasible due to lack of data since for some boreholes and acidizing steps the pump test was only carried out for one flow rate. As a result, no linear equation could be obtained for four boreholes (boreholes 11, 12, 13 and 14). Thus, an averaged slope was used for normalization in order to use a standardized method for all boreholes and to be able to increase the number of boreholes analyzed. The variance σ^2 of the slope of Eq. (6) is 0.066. Even though using an averaged slope leads to some minor distortion regarding the absolute values of specific capacity, it does not influence the values for the relative improvement of the specific capacity from one acidizing step to the next, which are of far more interest for this study.

Since for most boreholes and acidizing steps more than one specific capacity value was obtained from pump tests, the existing specific capacity and flow rate values of each acidizing step and each borehole were averaged to generate mean values. The resulting mean values for each acidizing step then served as starting points for the normalization. The result of this normalization can be seen in Fig. 3.

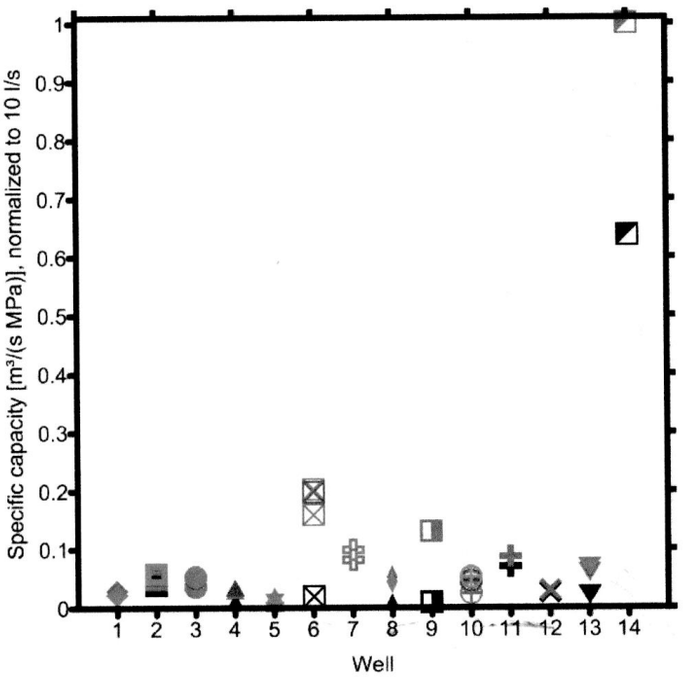

Figure 3. Specific capacity for different wells before and after acidizing (for details see Fig. 4). Colors indicate the time when the pump tests were performed: before first acid treatment (black), after first acid treatment (green), after second acid treatment (blue), after third acid treatment (red), after fourth acid treatment (orange), and after fifth acid treatment (pink).

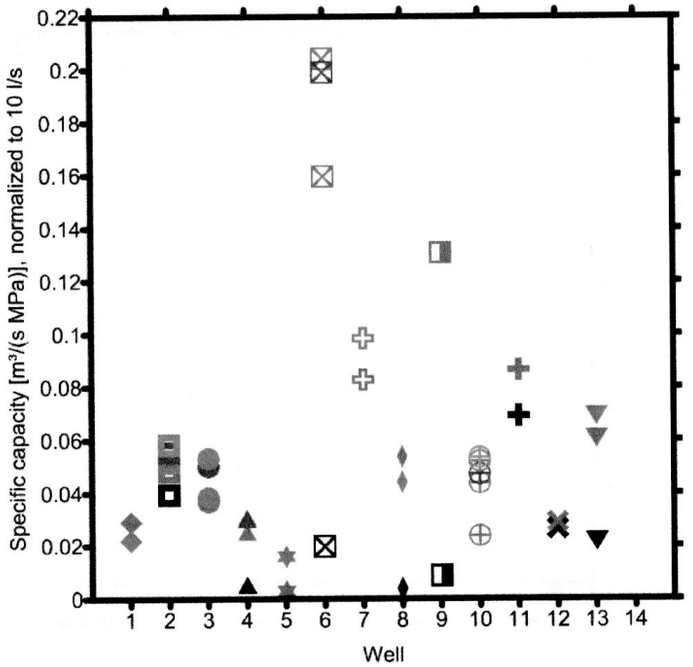

Figure 4. Specific capacity for different wells before and after acidizing (extract of Fig. 3). Colors indicate the time when the pump tests were performed: before first acid treatment (black), after first acid treatment (green), after second acid treatment (blue), after third acid treatment (red), after fourth acid treatment (orange), and after fifth acid treatment (pink).

The results of all pump tests were normalized to a flow rate of $10\,\mathrm{L\,s^{-1}}$ by using Eq. (6). A rate of $10\,\mathrm{L\,s^{-1}}$ is very low, much lower than the usual flow rate for most of the wells. It was chosen for two reasons. First of all, extrapolation to higher flow rates of, for example, $100\,\mathrm{L\,s^{-1}}$ can be problematic as it is unclear up to which flow rate the inferred linear equation holds true. As discussed above (Sect. 2), high flow rates are connected to the turbulent regime. Turbulence, however, implies that the exponential term of Eq. (5) comes to bear and, subsequently, the linear equation can no longer be used. The second reason for using a rather low value was the fact that some wells exhibit very low specific capacities. Extrapolating the linear equation to high flow rates would lead to negative values for these wells. As this is physically infeasible, it had to be avoided. Thus, a flow rate of $10\,\mathrm{L\,s^{-1}}$ met all requirements with regard to validity of extrapolation.

4 Results

In Fig. 3 the results of 14 boreholes are displayed, for which data for more than one acidizing step could be obtained. It should be noted that two boreholes of Fig. 2, wells 15 and 16, are not part of the group of these 14 boreholes for which all subsequent calculations and considerations are done.

In Fig. 3 some wells (namely wells 6, 9 and 14) exhibit an enormous increase in the specific capacity due to acidizing, while for the majority of wells acidizing only led to a marginal improvement. This latter observation becomes especially apparent in Fig. 4, which displays the same data as Fig. 3 with the exception of data for well 14. Thus, it is possible to show the small increases in specific capacity for all other wells in more detail. The fact that acidizing has only a small impact on some wells is especially pronounced for wells 2, 3 and 10. For these wells there are plenty of data for different acidizing steps. All these data show that the effect of the acidizing is diminished with increasing number of acidizing steps.

However, the improvement that is generated by acidizing depends not only on the number of acidizing steps, but also on the amount of acid used for each step. For some wells, the amount used was kept constant for different acidizing steps but some wells exhibit great variations (Table 1). In order to test how far the improvement of the specific capacity correlates with the amount of acid used, the specific capacity improvement was normalized to the amount of acid (15 % HCl) used. The results of this are shown in Fig. 5. In this figure, the changes in the specific capacity after an acidizing step, as compared to before the acidizing step, are displayed. Thus, only the relative improvement and not the absolute improvement is shown. This approach is used for all further comparisons. As could be expected, the improvement of the specific capacity is large for well 14 even after normalization to the amount of acid used. Moreover, it is again made evident that the effectiveness of the acidizing is reduced with every

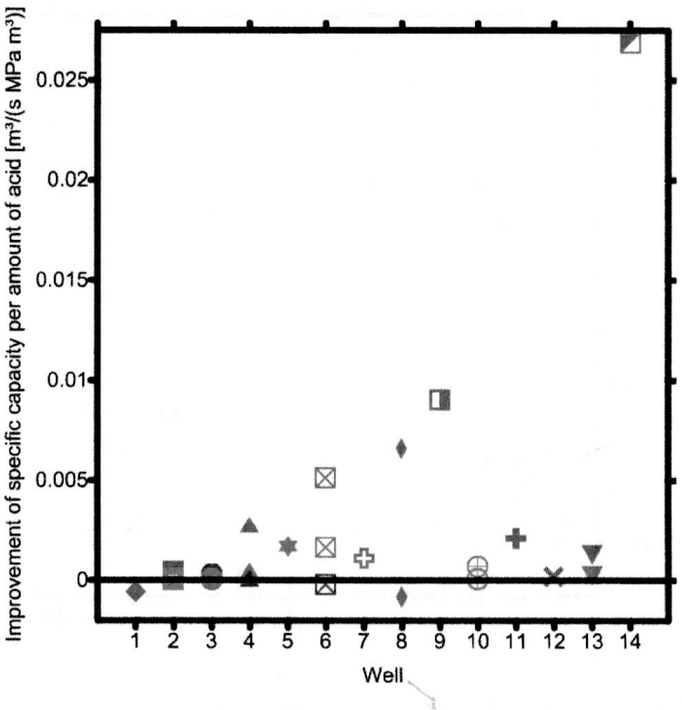

Figure 5. Improvement of the specific capacity normalized to the amount of acid used (for details see Fig. 7). Colors indicate the acidizing step that causes the improvement: first (green), second (blue), third (red), fourth (orange), and fifth (pink).

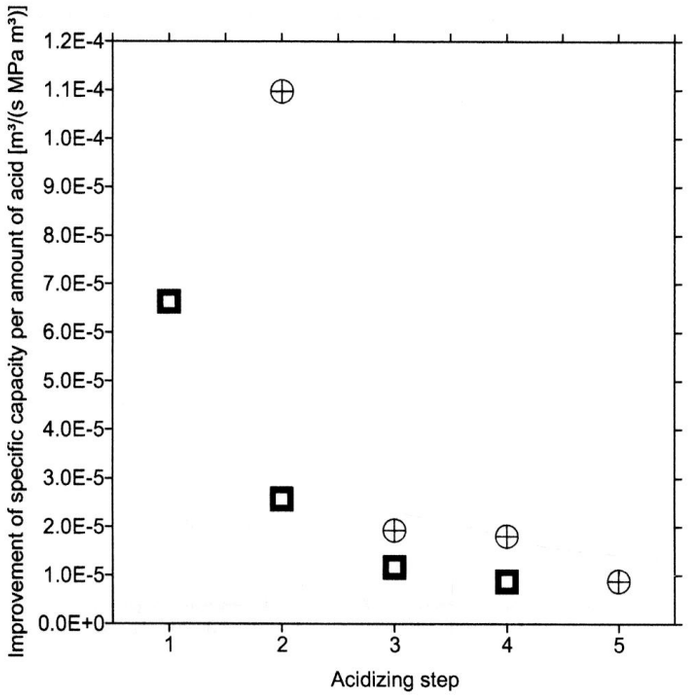

Figure 6. Improvement of the specific capacity normalized to the amount of acid used for two wells: well 2 (black squares) and well 10 (black crossed circles).

further acidizing undertaken. Thus, the trend that could already be observed in Fig. 4 holds true even if the amount of acid used is taken into account.

It becomes even clearer in Fig. 6, where the increase in specific capacity per acidizing step has been plotted for two wells. Wells 2 and 10 are those that exhibit the highest number of acidizing steps undertaken and monitored, and they therefore provide the best database. However, even for those two wells the data are not perfect. For well 10 the specific capacity of the unstimulated well has not been measured, and thus the improvement due to the first acid treatment is unknown. Still, the trend of initially high gains due to acidizing with subsequent stagnation at low levels is apparent.

Except for well 14, there are some other wells that exhibit a significant improvement of the specific capacity. These are primarily wells that already displayed a large improvement in Fig. 4; however, well 8 is an exception to this rule. For this well, the first acid treatment was extremely effective, while the second acid treatment shows a surprising result: the specific capacity decreased. Thus, the second acid treatment worsened the well compared to the situation after the first acid treatment. If this were the only well for which such an observation could be made, an error in the recorded pump test data or a mistake in its analysis would have been a likely explanation for this unexpected result. However, three other wells, namely wells 1, 4 and 6, exhibit a similar behavior. This can be observed in Fig. 7, which is an extract of Fig. 5 and shows the results in more detail.

In this figure it is very obvious that for some wells continued acidizing results in a reduction of the specific capacity. The first and maybe second acid treatment lead to an improvement of the specific capacity, but subsequent acidizing worsens the results. In all cases in which the initial specific capacity is known, acidizing was successful (i.e., the specific capacity after the last acidizing step was higher than initially), even for wells that show a reduction after the first or second acidizing step. However, in some cases the result could have been better if less acid treatments had been applied.

In Fig. 8 the improvement of the specific capacity in percent is shown. Again it is normalized to the amount of acid used, and in this case also to a flow rate of $10\,\mathrm{L\,s^{-1}}$. The latter normalization is necessary as percentages are based on absolute values and therefore need to have the same reference value if they are to be compared.

As in all other figures, the improvement is not related to the initial specific capacity but to that of the acidizing step before. In the case of percentages, this means that some wells exhibit extremely high improvements of more than 25 % per m^3 acid. However, in general, these wells were suffering from very low initial specific capacities so that even moderate improvements translated into high percentage gains.

Nevertheless, it is noteworthy that wells that show a reduction in specific capacity with consecutive acidizing (wells 4, 6 and 8) are among the group of wells that show high initial percentage gains. Unfortunately, there are no data for wells 1, 5 or 9, which could indicate if this is a pattern or a mere

此为试读，需要完整PDF请访问：www.ertongbook.com